Tribological comparison of different C-based coatings in lubricated and unlubricated conditions

I. Ciarsolo[1], X. Fernandez[1], U. Ruiz de Gopegui[1], C. Zubizarreta[1], M.D. Abad[2,‡], A. Mariscal[2], I. Caretti[3], I. Jiménez[3], J.C. Sánchez-López[2,*]

[1] IK4-Tekniker, Polo Tecnológico de Guipúzcoa, Calle Iñaki Goenaga 5, 20600 Eibar, Spain

[2] Instituto de Ciencia de Materiales de Sevilla (CSIC-Univ. Sevilla), Avda. Américo Vespucio 49, 41092 Sevilla, Spain

[3] Instituto de Ciencia de Materiales de Madrid (CSIC), Sor Juana Inés de la Cruz, 28049 Cantoblanco, Madrid, Spain

e-mail: jcslopez@icmse.csic.es

Abstract

The use of carbon-based coatings (hydrogenated and non-hydrogenated DLC, doped and alloyed-DLC) is of a wide interest due to its applications in mechanical components submitted to friction and wear including sliding parts in automotive engines. A tribological comparative analysis using a reciprocating (SRV) tester in lubricated and unlubricated conditions with a 4-stroke motor oil has been carried out on six currently relevant state-of-the-art coatings (namely WC/a-C, TiBC/a-C and TiC/a-C:H nanocomposites, Ti-doped DLC, BCN film and a crystalline monolithic TiC film as reference). The quantification of the fraction of the sp^2-bonded matrix has been done by fitting of C1s XPS peak and the mechanical properties evaluated by nanoindentation.

‡Current address: Department of Nuclear Engineering, University of California – Berkeley, Etcheverry Hall, 2521 Hearst Avenue, Berkeley, California 94720-1731, USA

The comparative analysis has allowed us to identify the capabilities of each system depending on the testing conditions and the possible synergies as a function of the chemical composition and film nature. Under lubricated harsh conditions (max. contact pressure 1.7 GPa) only coatings displaying hardness superior to 20 GPa could stand the sliding motion without failure. At lower contact pressures, a significant fraction of sp^2 carbon (≥75%) is advantageous for reducing wear in boundary lubrication. WC/a-C, BCN and Ti-DLC films showed the best tribological response in dry sliding conditions. This fundamental information would be of relevance for assisting engineers in selecting best partnership for lubrication systems.

1. Introduction

Hard carbon coatings display a number of highly interesting material properties that have led to their use in a wide range of tribological applications. Their high hardness, corrosion and wear resistance, and their low friction allow using them as protective layers on bearings, gears and engine components [1-4]. In many aspects, the demands on coatings for machine components are tougher than those for cutting tools [5]. The expected lifetime is very long, the coating costs must normally be low compared to component costs, the substrate hardness is rather low, failure or detachment of the coating can lead to catastrophic failure of the whole system and usually the contact is lubricated. For the last three decades, solid lubrication by thin coatings has mainly been used to stretch the limits of classical oils and/or fluid-base lubricants [6].

Coating of the working surface with diamond-like carbon (DLC) films gives similar frictional properties and excellent protection against transfer of countermaterial to the working surface, even in the case of base oil without any additives [7]. DLC is an

amorphous carbon (a-C) or hydrogenated amorphous carbon (a-C:H) film material with a high fraction of metastable sp^3 carbon bonding. Among different categories, doped and alloyed-DLC have the capacity to meet the increasingly stringent application requirements of advanced mechanical systems [2]. Although enhancement of the hardness is in principle desired the generation of internal compressive stress, particularly in coatings with high sp^3/sp^2 ratios, favours the film delamination. The accumulation of compressive stresses in DLC films have been currently overcome by doping with metallic elements or using gradient functional underlayers. New elements incorporated into a-C(H) coatings can either be diluted in the matrix, and a new single phase coating is produced, or be present as a second separate phase modulated in the nanometer scale to form multilayers or nanocomposites. Doped-DLC (with metals like Ti, Ta, Nb, Cr, etc. or non-metals like B, N, Si or F) belong to the first family whilst metal carbides (MeC) nanocrystals dispersed in a-C(H) matrixes are good examples of the second one. This generation of multicomponent nanocomposite coatings opens new possibilities of property improvement by appropriate control of their composition and structure at the nanoscale [8-10].

MeC/a-C:(H) coatings have been found to prevent fracture under severe load by the presence of the amorphous boundary phase that facilitates grain boundary sliding [10]. The estimation of the ratio between the nanocrystalline and the amorphous phases has been proved to be essential to correlate the tribological properties with the film composition [8] although is not generally assessed in the published works.

Boron/carbon/nitrogen (BCN) compounds based on the graphite network are one of the carbon alloys and a kind of hybrids of graphite and hexagonal boron nitride (h-BN). Ternary BCN films, although softer than B_xC compounds, combine a good friction

coefficient, adhesion and wear resistance [11-12]. Moreover, increased thermal stability over a-C and a-CN up to 800ºC has been demonstrated [13].

With the introduction of DLC and related carbon compound coatings in existing systems the major concern for their successful application is to ensure a reliable performance under dry and oil-lubricated conditions. In this sense, intensive research is devoted to study the synergies between carbon-based coatings and new environment-friendly additives for lubricants [14-16] in order to exploit them in partnership. However, most previous works has tended to focus mainly on model formulations containing either one particular additive or combination of two, and not with fully formulated oils, which in reality are employed in most applications. To prospect this, an overview of relevant examples of current state-of-the art materials under diverse contact conditions would be useful to deduce the influence of the phase composition on their tribological performance. Normally, the coating materials are studied separately under different testing conditions, substrates and type of tribometers, which makes difficult the establishment of correlations. In this work, a comparative analysis will be carried out on relevant carbonaceous material coatings including amorphous or nanostructured composition, monolithic or multicomponent nature. They will be tested in a SRV tribometer under different testing conditions, including liquid (fully formulated oil) or solid lubrication, in order to get knowledge about the best systems and possibilities of these carbon-based coatings to be fully exploited in mechanical components.

2. Experimental details

2.1. Coating deposition

Six different carbon-based coatings of different nature and composition were selected for this tribological study: three metal carbide/amorphous carbon nanocomposites (WC/a-C, TiBC/a-C and TiC/a-C:H), a Ti-doped DLC coating, an amorphous monolithic BCN film and a crystalline monolithic TiC film as reference. The coatings were deposited on mirror-polished M2 steel of 24 mm of diameter. Table 1 summarizes the set of coatings together with their chemical and physical properties. The elemental chemical composition has been determined by X-ray photoelectron spectroscopy (XPS). The total thickness includes the buffer interlayer commonly deposited to increase the adhesion to the steel substrate, whose composition is indicated in the same table.

The synthesis of the WC/a-C and TiBC/a-C films was carried out in a high vacuum chamber at an initial pressure of 3×10^{-4} Pa by co-sputtering of graphite and a second target (WC or a composite ceramic (60:40) TiC:TiB_2) in 0.60 Pa of argon. The substrates were mounted in a rotary sample-holder situated at 10 cm from the target. The temperature was found to vary in the range of 150–200 °C under the effect of the plasma as measured by a thermocouple. A negative bias of 100 V was applied to the substrates for the TiBC/a-C system. Applied sputtering powers were 150 W (WC); 125 W (TiC:TiB_2) and 250/300 W for the graphite. Further details about the synthesis procedure can be found in the following references: WC/a-C [17], TiBC/a-C [18].

The BCN coating [12] was deposited at room temperature by ion beam assisted deposition, by using two electron gun evaporators as sources of B and C atoms (AP and T CARRERA, mod. EVM-5 and EV1-8) and a Kauffman ion gun (Commonwealth Scientific, mod IBS) for assistance with N_2 gas, installed in a high vacuum chamber with 1×10^{-4} Pa base pressure. Simultaneous impinging fluxes of 4×10^{15} at/cm^2·s, 4×10^{15} at/cm$^{2\cdot}$s and 1×10^{15} ions/cm^2·s for B, C and N, respectively, were used in accordance with previous results [19]. The evaporators were run at a power of 700 W for B and

1500 W for C. Assistance was performed at 50° incident angle with a N_2^+ ion current of 0.16 mA/cm^2 at 500 eV. The working pressure was kept constant at 0.01 Pa. A ~1µm thick Ti(N) interlayer was deposited on the M2 steel substrate to avoid the formation of brittle Fe_xB compounds and improve the adhesion of the BCN coating. The gradient Ti(N) layer was grown by evaporation of Ti and increasing N_2^+ ion assistance current [12].

The TiC/a-C:H and TiC films were deposited by reactive magnetron sputtering using C_2H_2 as carbon precursor and a titanium target in a vacuum chamber evacuated up to a pressure of 0.01 Pa. A DC-pulsed (250 KHz) ENI-RPG50 plasma source has been used together with an auxiliary arc source with distant anode to enrich the plasma. The substrates were heated by means of infrared radiant heaters up to 500 ºC followed by an Ar/H_2 glow discharge cleaning at a pressure between 0.4 and 0.8 Pa. The TiC/a-C:H film was deposited with a power density of 6.3 W/cm^2 and a bias voltage of 50 V. A gradient Ti/TiC underlayer was previously deposited varying the bias from 500 to 50 V. During the deposition process, the argon flow was constant (65 sccm) and the C_2H_2 flow was 20 sccm. The pressure in the chamber during the deposition process was set to values in the range of 0.2-0.7 Pa. The TiC film was deposited with a power density of 5.6 W/cm^2 and a bias voltage of 50 V. During the deposition process, the argon flow was constant (65 sccm) and the C_2H_2 flow was 7 sccm.

The Ti-DLC film was deposited by cathodic arc evaporation in the industrial equipment MIDAS 775 (designed and manufactured by IK4-Tekniker) using C_2H_2 and a titanium target [20,21]. This system has 12 circular evaporators of 100 mm, working intensity range of 60-200 A, and a 45 kW pulsed DC bias power supply system consisting of two MDX II DC and one SPARC-VS pulsing unit from Advanced Energy. Prior the coating deposition process, the samples were submitted to the same pre-treatment process than

TiC/a-C:H and TiC films. To improve the coating adhesion a pure titanium interlayer (around 1 μm thickness) was deposited using a high bias voltage of 1000 V. Then, the Ti-DLC coating was completed by adding the necessary reactive gases, Ar (200 sccm) and C_2H_2 (200 sccm) measured with a mass flow controller from Bronkhorst High Tech. During this step the pressure in the chamber was found to be in the range of 0.2-0.8 Pa. The arc intensity of the titanium target was set at 75 A and the bias voltage at 30 V.

2.2. Coating characterization

Scanning electron microscopy (SEM) data were recorded in a FEG Hitachi S5200 microscope operating at 5 kV. The arithmetical average surface roughness (Ra) was evaluated by means of a stylus profilometer. Raman spectra measurements (200-2000 cm^{-1}) were carried out with a LabRAM (Horiba Jobin Yvon) spectrometer equipped with a true confocal microscope, a charge-coupled device detector and a He-Ne laser (532 nm) working at 5 mW to avoid sample damaging. All the samples were analysed with 100 s exposure times and aperture openings of 100 μm using a 100× magnification. No background subtraction is applied to the Raman spectra. The crystal structure of the films was examined by grazing incidence X-ray diffraction (XRD) using an angle of 5º and Cu Kα radiation in a Siemens D5000 diffractometer with parallel beam geometry. A step size of 0.02 (2θ) with 10 s per point were used. XPS measurements were carried out using two spectrometers. A VG-Escalab 210 spectrometer working in constant analyzer energy mode at a pass energy of 50 eV and non-monochromatic Mg K_α ($h\upsilon$=1253.6 eV) radiation as excitation source was used for measuring the WC/a-C, TiBC/a-C and BCN samples. A Thermo Scientific K-Alpha ESCA instrument equipped

with aluminium $K_{\alpha 1,2}$ monochromatized radiation at 1486.6 eV X-ray source was used for the remaining samples (TiC/a-C:H, Ti-DLC and TiC). Photoelectrons were collected from a take-off angle of 90° relative to the sample surface. The measurement was done in a constant analyser energy mode with 20 eV pass energy for high resolution spectra. Charge referencing was done by setting the binding energy of the sp^2 C-C(H) component of the C 1s photoelectron peak at 284.5 or 285.0 eV. Samples were previously cleaned using Ar^+ ion bombardment at (2.5×10^{-3} Pa; 2.5 kV; 1.7 μA/cm^2; 300 s). These conditions were found as most appropriate to remove preferentially the hydrocarbon surface contamination layer without affecting the film elemental composition. Quantification was accomplished by determining the elemental peak areas, following a Shirley background subtraction and accounting for the relative sensitivities of the elements using Scofield cross-sections. Fitting analysis was then carried by a least squares routine on the C1 s peak of the films to estimate the relative amount of the different carbon bondings (carbides and amorphous carbon) in agreement with previous works [9,17,18,22]. A Gaussian-Lorentzian ratio of 0.7-0.8 was used and FHWM values were fixed at the following values for the different components: C-C(H) (1.7-1.8), Ti-C (1.5), C-O (2.2.-2.5), C-N (sp^2) (2.2); C-N (sp^3) (2.5). The narrow peak originated by the C-Ti bonding in the pure TiC film was necessary to be reduced to 0.7.

Hardness measurements were performed with a Nanoindenter II (Nano Instruments, Inc., Knoxville, TN) with a diamond Berkovich (three-sided pyramid) indenter tip in the continuous stiffness measurement mode and a Fischer nanoindenter equipment with Vickers indenter. In both cases, the load–displacement data were analyzed using the method of Oliver and Pharr to determine the hardness and the elastic modulus as a function of the displacement of the indenter. The maximum load was selected in such a

way that the maximum indentation depth did not exceed 10–15% of the coating thickness in order to avoid the influence of the substrate.

The tribological characterization was carried out in a reciprocating (SRV) tribometer using a ball-on-disk configuration in lubricated and unlubricated conditions between coated disks and steel balls. The used lubricant was a 4-stroke fully synthetic motor oil (SuperSyn Mobil 5W50). According to the supplier, the kinematic viscosity of the oil is 104.6 mm^2/s at 40 ºC and 17.4 mm^2/s at 100 ºC. Before the test, the contact region was wetted with a drop of lubricant (∼0.3 ml). No further addition is done during the SRV sliding test. For each condition (lubricated and non-lubricated), two different sets of testing parameters (load, frequency, stroke and duration) were used. The different conditions were chosen in order to have a stable friction coefficient and a measurable wear for all the studied coatings. A detailed summary is displayed in Table 2. The temperature was fixed at 50 °C for all the tests. Two identical tests were carried out for each condition. The average friction coefficient was measured throughout the test and normalized wear rates of the counterfaces [worn volume (mm^3) / (sliding distance (m) × applied load (N))] were evaluated after completion of the test by PLμ Optical Imaging Profiler. Normalized ball wear rates were evaluated after examination of the balls and calculation of the worn volume using the spherical cap equation. Normalized film wear rates were calculated by numerical integration of the cross-section areas along the film track.

3. Results and discussion

3.1. Microstructural and chemical characterization of the initial films

The microstructure of the coatings was studied by SEM examination of cross-sectional views carried out on silicon pieces. A representative micrograph is shown in Fig. 1 for each type of coating. A bilayer structure is generally observed as a consequence of the previous deposition of an adhesion interlayer, whose thickness goes from several hundred of nm to above 1 μm. A columnar growth is clearly developed in all the coatings except in the TiBC/a-C and BCN. The formation of ternary compounds by introduction of boron atoms has reduced the columnar growth and promoted dense structures.

The crystalline composition was analyzed by means of grazing incidence XRD. Fig. 2 shows the XRD patterns for the samples under study. From the broadening of the main peak, average crystallite sizes were determined using the Scherrer formula (see Table 1). The diffraction pattern of the WC/a-C film exhibit mainly a broad peak located at ≈38° which can be associated with the (111) reflection peak of the fcc β-WC_{1-x} phase. The diffractogram shown for the TiBC/a-C coating reveals a broad band at 35°. This peak is between the (100) TiB_2 and (111) TiC planes. A mixture of both components and the formation of a ternary phase including titanium, carbon and boron (TiB_xC_y) are at the origin of this peak, as demonstrated by XANES [23]. In the TiC/a-C:H and TiC coatings, the characteristic (100), (111) and (220) diffraction peaks from cubic TiC phase were identified together with some peaks originated by a titanium underlayer and Fe from the substrate. Finally, the Ti-DLC and BCN coatings were XRD amorphous and only the peaks due to the grown underlayers (Ti and gradient TiN-based, respectively) were observed.

The formation of an amorphous carbon bonded-matrix is confirmed by Raman spectroscopy (Fig. 3) for all the carbonaceous coatings. The presence of the two peaks characteristic of the sp^2 sites of all disordered carbons at 1350 (D-peak) and ordered

graphite at 1585 cm^{-1} (G peak) are clearly observed except in the monolithic TiC, as expected. In this latter case, some peaks are detected in the range of 450–750 cm^{-1}. These vibrational modes are indicative of understoichiometric titanium carbide. It should be mentioned that stoichiometric TiC has no Raman vibration modes but the introduction of disorder due to carbon vacancies makes them active [11]. The D and G bands appear more resolved and intense in the case of carbon incorporation by using acetylene (TiC/a-C:H and Ti-DLC) as precursor as compared to the non-reactive sputtering of graphite targets. This result indicates a higher degree or ordering of the sp^2 aromatic domains in the carbon matrix.

In order to estimate the relative amount of sp^2-bonded C with respect to the total carbon content (i.e. lubricant fraction) the measurement of the C 1s photoelectron peak has been used. XPS is sensitive to the local coordination about the excited atom (i.e. carbon in this case), being appropriate to evaluate the fraction of carbon atoms in each chemical bonding (C-C, C-N or metal-(B)-C). The C 1s peak was fitted assuming main contributions from Ti-C (282.0-282.5 eV), Ti-B-C (283.2 eV), W-C (283.5 eV), sp^2 C-C (284.5-285.0 eV) [11,12,17,18], sp^2 C-N (285.8 eV), sp^3 C-N (287.7) [23]. In addition, C-O contributions were included in the high binding energy side due to the presence of oxygen impurities. Figure 4 shows the C 1s XPS peaks for the selected coatings and the fitting of the different components present in the samples. This analysis allowed to estimate the fraction of amorphous sp^2-C bonded matrix [$X_{C(sp^2)}$] with respect to the total atoms as depicted in Fig. 5 and Table 1. Three groups of samples can be distinguished attending to the $X_{C(sp^2)}$ content: almost absent (monolithic TiC; 10%); medium (nanocomposites WC/a-C and TiBC/a-C; 41-43%) and high (BCN, TiC/a-C:H and Ti-DLC; 75-89%).

The film characterization was completed with the measurement of the mechanical properties (Hardness and reduced Young modulus) by nanoindentation. The obtained values are summarized in Table 1 and represented in Fig. 6. The hardness values range from 8 GPa (for the Ti-DLC coating) to 26 GPa (for the ceramic monolithic TiC). The metal carbide/amorphous carbon composites exhibit intermediate values of about 16 to 22 GPa indicative of the mixture of nanocrystalline hard (MeC) and soft amorphous a-C(H) phases. The BCN despite of its amorphous nature shows a reasonable hardness (18 GPa) based on the covalent bonding characteristic of the BCN networks [15] including C-N and B-N bonds.

3.2. SRV Tribological characterization

The set of coatings were submitted to tribological evaluation under 4 different conditions (lubricated and non-lubricated at two different loads/frequencies) for a comparative analysis. The values of average friction coefficient and the measured specific wear rates are shown in Fig. 7.

For the lubricated tests in the most severe conditions (50 N; 100 mm/s; 50 Hz; 30 min), only two coatings (TiBC/a-C and TiC) could withstand the test without film failure or delamination. The estimation of the film wear tracks in the lubricated tests was difficult to measure and consequently the worn ball volume was measured instead. When decreasing the load to 20 N and frequency to 25 Hz, most of the coatings could be measured keeping the friction between the counterfaces reduced. In general, the average friction coefficient is similar under lubricated conditions, in the range of 0.11-0.12, independently of the coating type. This is indicating that in this situation the friction forces are more determined by the surface chemistry rather than topography. However,

the coating material has influenced the mechanical response of the interacting surfaces depending on the testing conditions. Thus, under harsh conditions, a high load-bearing capacity is needed and only the hardest coatings TiBC/a-C and TiC, with 22 and 26 GPa respectively, could resist the tribological test. However, by halving the severity of the test the presence of a significant fraction of amorphous carbon phase yields a improved wear performance. The coatings BCN and Ti-DLC with higher $X_{C(sp^2)}$, approximately 89%, demonstrated the best performance, followed by the TiC/a-C(H) with $X_{C(sp^2)}$=75% (cf. Fig. 4). It has been previously reported that DLC/steel combination gives more efficient running-in process, less wear and up to 25% lower steady-state friction than the DLC/DLC and steel/steel combinations [24]. Under boundary lubrication conditions, the formation of tribochemical films (so-called tribofilm) on the contact surfaces protects metallic surfaces from wear. Such films are generated by tribologically activated reactions between lubricant additives (friction modifiers, anti-wear and extreme pressures) and the metallic surface [25]. However, when the surface is coated by an inert low-friction carbon-based coating, the mechanism of conventional additives may be hindered or even prevented. This is generally the case when both contact parts are coated by DLC or DLC/steel combinations, at least at low additive concentration [14,16,26-28]. In these conditions, no evidences of reaction products or tribofilm formations were found, with a carbon transfer layer, responsible for low-friction behaviour and low wear behaviour of DLC/steel systems. Vengudusamy et al., in his recent work [29], suggests that under fully formulated lubricated conditions additives form initially a tribofilm on the steel ball, followed by transfer (although moderate) of C from the DLC film. These BCN and Ti-DLC coatings have higher sp^2-C bonded fractions, reproducing the behavior demonstrated by DLC/steel tribopairs. The remaining samples have an $X_{C(sp^2)}$ fraction below 50% and resulting higher hardness.

The major fraction of hard phases (WC, TiBC and TiC) in these coatings would difficult the transfer film build-up and steady-state, and consequently, exhibit lower performance in the presence of additives.

In dry sliding conditions at contact pressures of the order of 1 GPa, the solid surfaces move so close each other that there is considerable asperity interaction and the tribological behaviour is determined primarily by the coating properties. The first conclusion that can be obtained from Fig. 7 (bottom, UNLUB) is the parallelism between the friction coefficient and the film endurance, confirming this hypothesis. Thus, lower friction coefficients are associated to lower specific wear rates. The WC/a-C nanocomposite and the amorphous BCN coatings afforded the best results both in terms of friction coefficient and wear resistance under low and high frequencies (2 and 10 Hz) followed by the Ti-DLC sample. The friction coefficients are found to be 0.11, 0.16 and ~0.2, respectively. The remaining coatings (TiBC/a-C, TiC/a-C:H and TiC) gave values above 0.2. Concerning the wear performance, the comparison of the wear rate values obtained at 10 Hz frequency puts in evidence the excellent result denoted by the amorphous monolithic BCN film (~1×10^{-7} mm^3/Nm), followed closely by the WC/a-C and Ti-DLC films (~4×10^{-7} mm^3/Nm). In the last group, TiBC/a-C, TiC/a-C:H and TiC gave k values in the order of 10^{-6} mm^3/Nm. Similar trend can be extracted from the graph obtained from the measures at 2 Hz although the differences are more remarkable owing to the limited sliding distance (4,8 m). In the initial stages, the wear rate is higher and gradually decreases until a steady-state is reached.

These results are in agreement with the estimated fraction of amorphous sp^2-C excepting WC/a-C whose value is significantly lower. The ability of DLC and carbon-based nanocomposite compounds to form low shear strength graphitic-like layers in the contact interface is very well known [2,11,12]. The exception of WC/a-C

nanocomposite film can be likely attributed to the decomposition of non-stoichiometric WC_{1-x} phases under friction generating a-C into the contact and thereby decreasing friction as demonstrated in [12]. The metal carbide/amorphous carbon composite represents a good blend of tribological and mechanical properties provided by their microstructure formed by a mixture of hard nanocrystals (that gives mechanical strength) and amorphous ductile phase (that provides lubricity). The wear performance found in this paper is similar to that determined previously in MeC/a-C nanocomposite films using a pin-on-disk tribometer [9]. In this latter work, the wear resistance increased in the sequence TiBC<TiC<<WC. Despite of the improvement in hardness, the higher brittleness of the TiBC phases leads to film cracking and increased wear.

The covalent BCN film is formed by a very amorphous graphite-like network with a significant fraction of C-N and B-N bonding increasing the cross-linking in combination with a high percentage of sp^2 carbon matrix. Despite a dominant three-fold coordination of the B, C, and N, hexagonal planes cannot be distinguished by TEM atoms in this type of material [30]. It is also possible that the thick hard Ti(N) interlayer in this system provides a good mechanical support to guarantee a low contact area although a good mechanical behavior has been previously reported for similar BCN compounds deposited on Si (100)[11]. The importance of a hard underlayer has been previously pointed out to be essential for extreme low friction [31]. Finally, the monolithic TiC represents a situation with a high mechanical strength but limited lubricant properties by the deficiency of sp^2-bonded C phase.

A possible influence of the surface roughness cannot be ruled out as the R_a values of the BCN and WC/a-C films are the lowest among them (cf. Table 1). This factor can contribute particularly at the initial stages before the asperities are soon worn flat. However, the range of measured values (8 to 29 nm) seems to be very small to explain

the variation of the friction coefficients measured in dry conditions. Previous works [32,33] have reported the influence of surface roughness in friction and wear rates for changes in several order of magnitude (i.e nm to μm). For instance, Svahn et al. [33] found that a variation of roughness from 7 to 390 nm was necessary to produce an increase of friction from 0.1 to 0.3 under non-lubricated conditions (variation of COFs comparable to here presented). Therefore, other factors are influencing the tribological behaviour although an initial contribution (before smoothening) cannot be ruled out.

In summary, the observed tribological behaviour can be understood as the result of a good compromise between hardness and lubricant properties as determined by the chemical composition and bonding nature.

3.3.Raman analysis of the wear tracks

To investigate the wear track chemistry and structural changes, phase composition of the worn surfaces was evaluated using micro-Raman spectroscopy. For each tested condition, those two samples displaying the best tribological behaviour were studied, as shown in Figure 8. Under lubricated conditions and high sliding frequency (Fig. 8a), no Raman signal could be detected indicating the absence of surface oxides or amorphous free carbon in the contact. In the case of lubricated test at 25 Hz, the measured spectra of Ti-DLC and BCN coatings are very similar to those obtained before the tribotest. These two films exhibit the typical D and G bands that apparently did not suffer any substantial modifications. In the unlubricated tests at 10 Hz, certain regions could be identified inside the wear tracks where debris particles appeared adhered forming spots or bands (Zone I). This transfer material has suffered structural modifications and oxidation as denoted by the narrowing of the D and G bands at 1350 and 1595 cm^{-1}, in

the BCN sample, and the appearance of a broad band at 695 cm^{-1}, in the case of the Ti-DLC, originated by amorphous iron oxides (γ-Fe_2O_3/Fe_3O_4) from the ball counterface [11]. In the other locations (Zone II) the spectra are found to be similar to the original films. The observation of modifications in the Raman spectra of certain zones of the contact region during unlubricated tests is indicative of interfacial sliding where two dry surfaces are in close contact and tribochemical modifications appear (oxidation or graphitization). However, for lubricated tests, the presence of a thin film of liquid lubricant enables the separation of the surfaces limiting the asperity interaction and surface modification. The spectra measured for the unlubricated tests at lower frequency (2 Hz) did not reveal significant changes of the coating structure and composition, probably due to their limited sliding distance and severity.

4. Conclusions

In the case of carbonaceous coating/steel contacts under lubricated conditions, the coatings with higher fraction of sp^2-C phase are giving the best wear performance but if a high load-carrying capacity is needed then a harder coating material is preferable. Under lubricated harsh conditions (max. contact pressure 1.7 GPa) only coatings displaying hardness superior to 20 GPa could stand the test without failure or delamination. At lower contact pressures a fraction of sp^2–bonded C $\geq$75 % resulted advantageous for reducing friction and wear by generation of low-friction carbon-based material in the contact. Likewise, in dry sliding conditionsthe best performance is observed for WC/a-C, BCN and Ti-DLC coatings that contributes to decrease the shear stress (friction below 0.2) maintaining an optimum wear endurance (10^{-7} mm^3/Nm) thanks to the build-up of a graphitic-like material. An increased ordering of the

amorphous sp^2-C fraction is detected by Raman analysis of the wear tracks as a result of shearing process during interfacial sliding.

Acknowledgements

The Spanish MEC (projects nº MAT2007-66881-C02-01; MAT2011-29074-C02-01 and CONSOLIDER FUNCOAT CSD2008-00023) is acknowledged for financial support. I. Caretti acknowledges support from CSIC through a JAE-Doc fellowship.

References

[1] J. Robertson, Diamond-like amorphous carbon, J. Mat. Sci. Eng. R-Reports 37 (2002) 129-281 (2002).

[2] J.C. Sánchez-López, A. Fernández, Doping and Alloying Effects on DLC coatings, in: C. Donnet, A. Erdemir (Eds.) Tribology of Diamond-like Carbon Films: fundamentals and applications, Springer, New York, 2008, 311-338.

[3] A. Erdemir, C. Donnet, Tribology of diamond-like carbon films: recent progress and future prospects, J. Phys. D Appl. Phys, 39 (2006) R311-R327.

[4] R. Hauert, An overview on the tribological behavior of diamond-like carbon in technical and medical applications, Tribol. Int. 11-12 (2004) 991-1003

[5] S. Hogmark, S. Jacobson, M. Larsson, U. Wiklund, Mechanical and tribological requirements and evaluation of coating composites, in: B. Bhushan (Eds.) Modern Tribology Handbook, CRC press, Boca Raton, Florida, 2000, pp. 931-960.

[6] B. Podgornik, Tribological behavior of DLC films in various lubrication regimes, in C. Donnet, A. Erdemir (Eds.) Tribology of Diamond-like Carbon Films: fundamentals and applications, Springer, New York (2008), pp. 410-453.

[7] B. Podgornik, S. Hogmark, O. Sandberg, Influence of the surface roughness and coating type on the galling properties of coated forming tool steel, Surf. Coat. Technol. 184 (2004) 338-348.

[8] J.C. Sánchez-López, D. Martínez-Martínez, C. López-Cartes, A. Fernández, Tribological behaviour of titanium carbide/amorphous carbon nanocomposite coatings: from macro to the micro-scale, Surf. Coat. Technol. 202 (2008) 4011-4018.

[9] J.C. Sánchez-López, D. Martínez-Martínez, M.D. Abad, A. Fernández, Metal carbide/amorphous C-based nanocomposite coatings for tribological applications, Surf. Coat. Technol. 204 (2009) 947-954.

[10] A.A. Voevodin, J.S. Zabinski, Supertough wear-resistant coatings with 'chameleon' surface adaptation, Thin Solid Films 370 (2000) 223-231.

[11] I. Caretti, I. Jiménez, Influence of carbon content and nitrogen vacancies on the bonding structure and mechanical performance of graphite-like BC_xN thin films, J. Appl. Phys. 112 (2012) 063525.

[12] I. Caretti, J.M. Albella, I. Jimenez, Tribological study of amorphous BC_4N coatings, Diamond Relat. Mater. 16 (2007) 63-67.

[13] R. Gago, I. Jiménez, I. García, J.M. Albella, Growth and characterisation of boron–carbon–nitrogen coatings obtained by ion beam assisted evaporation, Vacuum 64 (2002) 199-204.

[14] M.I. de Barros-Bouchet, J. M. Martin, T. Le-Mogne, B. Vacher, Boundary lubrication mechanisms of carbon coatings by MoDTC and ZDDP additives, Tribol. Int. 38 (2005) 257-264.

[15] A. Neville, A. Morina, T. Haque, Q. Voong, Compatibility between tribological surfaces and lubricant additives - How friction and wear reduction can be controlled by surface/lube synergies, Tribol. Int. 40 (2007) 1680-1695.

[16] B. Podgornik and J. Vizintin, Tribological reactions between oil additives and DLC coatings for automotive applications, Surf. Coat. Technol. 200 (2005) 1982-1989.

[17] B. Vengudusamy, A, Grafl, K. Preinfalk, Tribological properties of hydrogenated amorphous carbon under dry and lubricated conditions, Diamond Relat. Mater. 41 (2014) 53-64.

[17] M.D. Abad, M.A. Muñoz-Márquez, S. El Mrabet, A. Justo, J.C. Sánchez-López, Tailored synthesis of nanostructured WC/a-C coatings by dual magnetron sputtering, Surf. Coat. Technol. 204 (2010) 3490.

[18] M.D. Abad, J.C. Sánchez-López, M. Brizuela, A. García-Luis, D.V. Shtansky, Influence of carbon chemical bonding on the tribological behaviour of sputtered nanocomposite TiBC/a-C coatings, Thin Solid Films 518 (2010) 5546-5552.

[19] I. Caretti, I. Jiménez, J.M. Albella, BCN films with controlled composition obtained by the interaction between molecular beams of B and C with nitrogen ion beams, Diamond. Relat. Mater. 12 (2003) 1079-1083.

[20] J. Goikoetxea, U. Ruiz de Gopegui, K. Garmendia, A. Delgado, Arc evaporator and method for operating the evaporator, Patent number WO2010072850A1.

[21] V. Sáenz de Viteri, M.G. Barandika, U. Ruiz de Gopegui, R. Bayon, C. Zubizarreta, X. Fernandez, A. Igartua, F. Agullo-Rueda, Characterization of Ti-C-N coatings deposited on Ti6Al4V for biomedical applications, J. Inorg. Biochem. 117 (2012) 359-366.

[22] J.C. Sánchez-López, C. Donnet, F. Lefebvre, C. Fernández-Ramos, A. Fernández, Bonding structure in amorphous carbon nitride: NMR, EELS, XANES and XPS study,

J. Appl. Phys. 90 (2001) 675-691.

[23] M. D. Abad, R. Sanjines, J. L. Endrino, R. Gago, J. Andersson, J.C. Sanchez-Lopez, Identification of ternary phases in TiBC/a-C nanocomposite thin films: Influence on the electrical and optical properties, Plasma Process. Polym. 8 (2011) 579-588.

[24] B. Podgornik, S. Jacobson, S. Hogmark, DLC coating of boundary lubricated components – advantages of coating one of the contact surfaces rather than both or none, Tribol. Int. 36 (2003) 843.

[25] K. Varlot, M. Kasrai, G.M. Bancroft, E.S. Yamaguchi, P.R. Ryason, J. Igarashi, X-ray absorption study of antiwear films generated from ZDDP and borate micelles, Wear 249 (2001) 1029–1035.

[26] M. Kalin,J. Vizintin, J. Barriga, K. Vercammem, K. Van Acker, A. Arnsek, The effect of doping elements and oil additives on the tribological performance of boundary-lubricated DLC/DLC contacts, Tribo. Lett. 17 (2004) 679.

[27] B. Podgornik, S. Jacobson, S. Hogmark, Influence of EP and AW additives on the tribological behaviour of hard low friction coatings, Surf. Coat. Technol. 165 (2003) 168-175.

[28] B. Podgornik, D. Hren, J. Vizintin, Low friction behaviour of boundary-lubricated diamond-like carbon coatings containing tungsten, Thin Solid Films 476 (2005) 92-100.

[29] B. Vengudusamy, A. Grafl, K. Preinfalk, Tribological properties of hydrogenated amorphous carbon under dry and lubricated conditions, Diamond Relat. Mater. 41 (2014) 53-64.

[30] I. Caretti, R. Torres, R. Gago, A. R. Landa-Cánovas, I. Jiménez, Effect of carbon incorporation on the microstructure of BCxN (x=0.25, 1, and 4) ternary solid solutions studied by transmission electron microscopy, Chem. Mater. 22 (2010) 1949-1951.

[31] D.V. Shtansky, T. B. Lobova, V. Yu. Fominski, S.A. Kulinich, I.V. Lyasotsky, M.I. Petrzhik, E.A. Levashov, J.J. Moore, Structure and tribological properties of WSe_x, WSe_x/TiN, WSe_x/TiCN and WSe_x/TiSiN coatings, Surf. Coat. Technol. 183 (2004) 328-336 (2004).

[32] J. Jiang and R.D. Arnell, The effect of substrate surface roughness on the wear of DLC coatings, Wear 239 (2000) 1-9.

[33] F. Svahn, Å. Kassman-Rudolphi, E. Wallén, The influence of surface roughness on friction and wear of machine element coatings. Wear 254 (2003) 1092-1098.

Figure captions

Figure 1. SEM cross-section views of the C-based coatings under study.

Figure 2. Grazing angle XRD diffractograms of carbon-based coatings deposited on steel.

Figure 3. Raman spectra of the as-deposited coatings under study.

Figure 4. Deconvolution of the C1s photoelectron peaks showing the different fraction of sp^2 C inside the coatings.

Figure 5. Fraction of sp^2 C [$X_{C\,(sp^2)}$] obtained by XPS of the different coatings.

Figure 6. Hardness and reduced Young Modulus of the different samples.

Figure 7. Average friction coefficient and specific wear rate values for the carbon-based coatings after tribological tests (lubricated LUB; unlubricated UNLUB; the value denotes the used frequency).

Figure 8. Raman analysis of the wear tracks of the two best tribological response of tested carbon-based coatings in each studied condition (lubricated LUB; unlubricated UNLUB; the value denotes the used frequency).

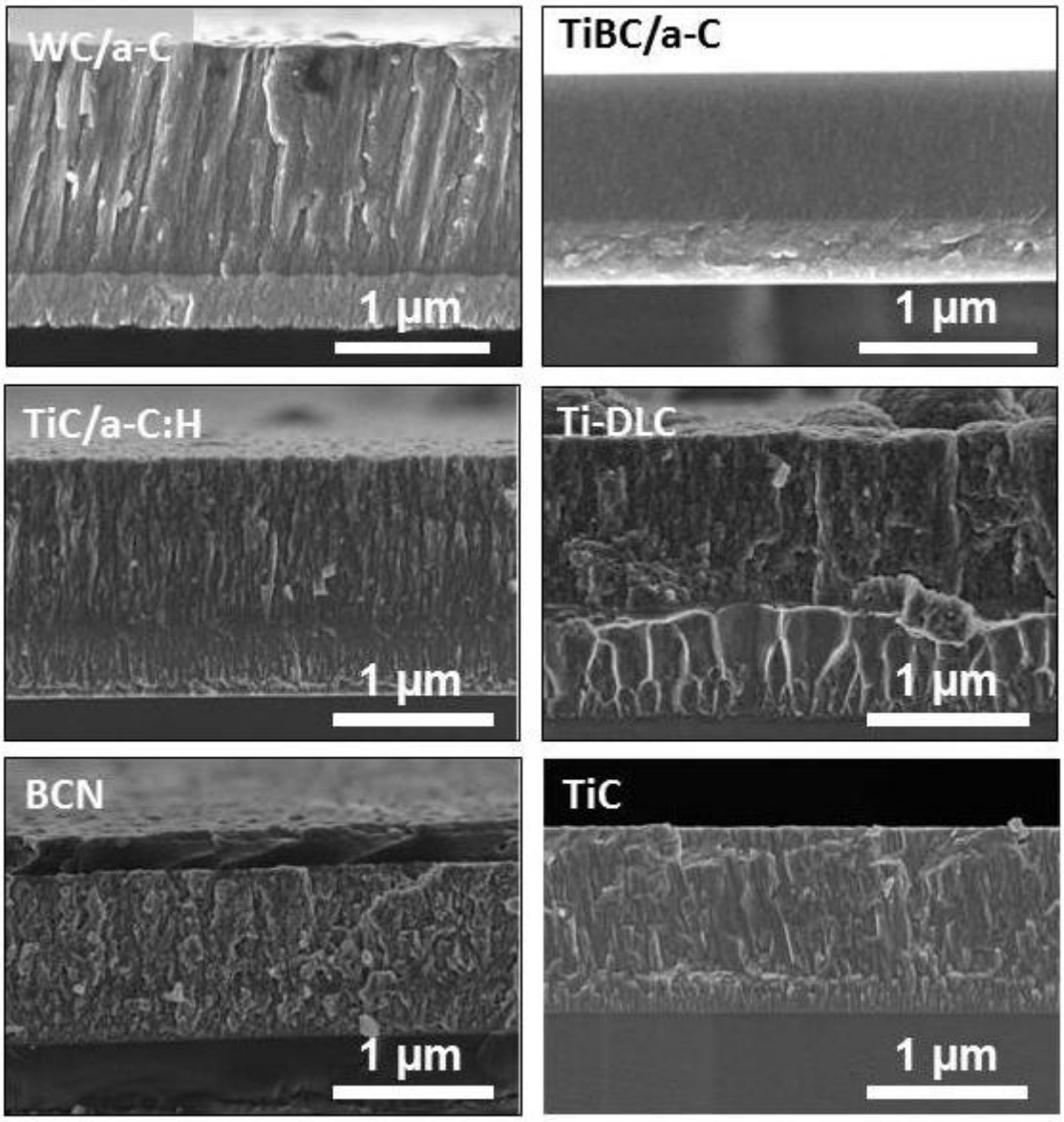

Figure 2

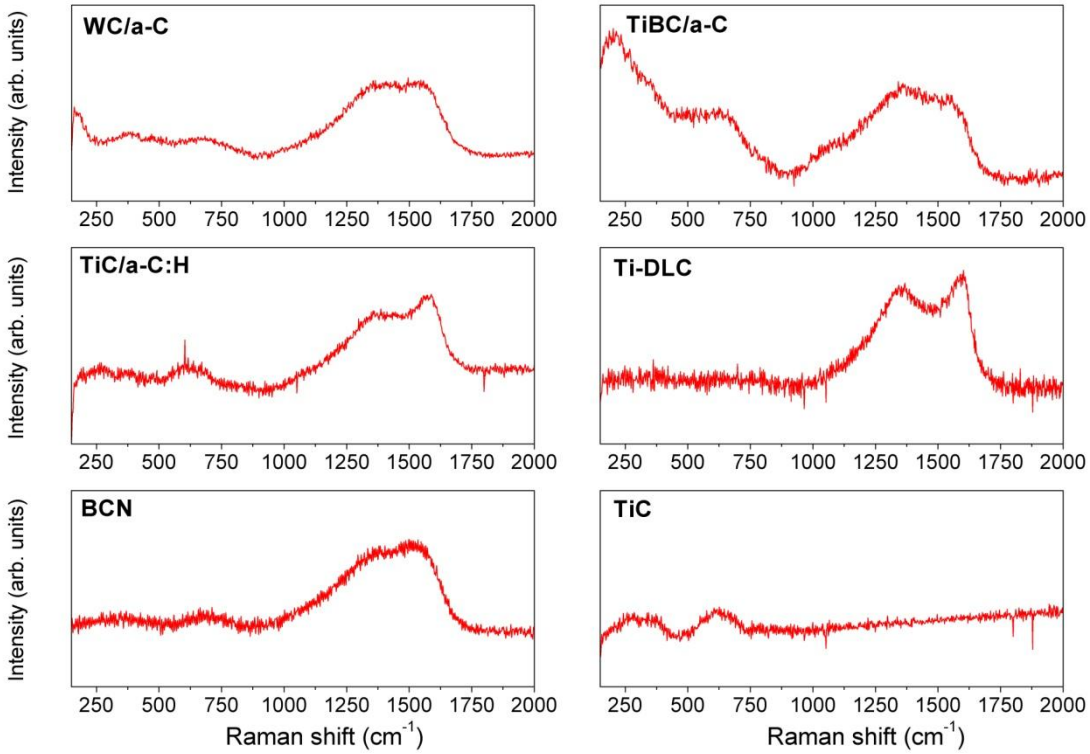

Figure 3

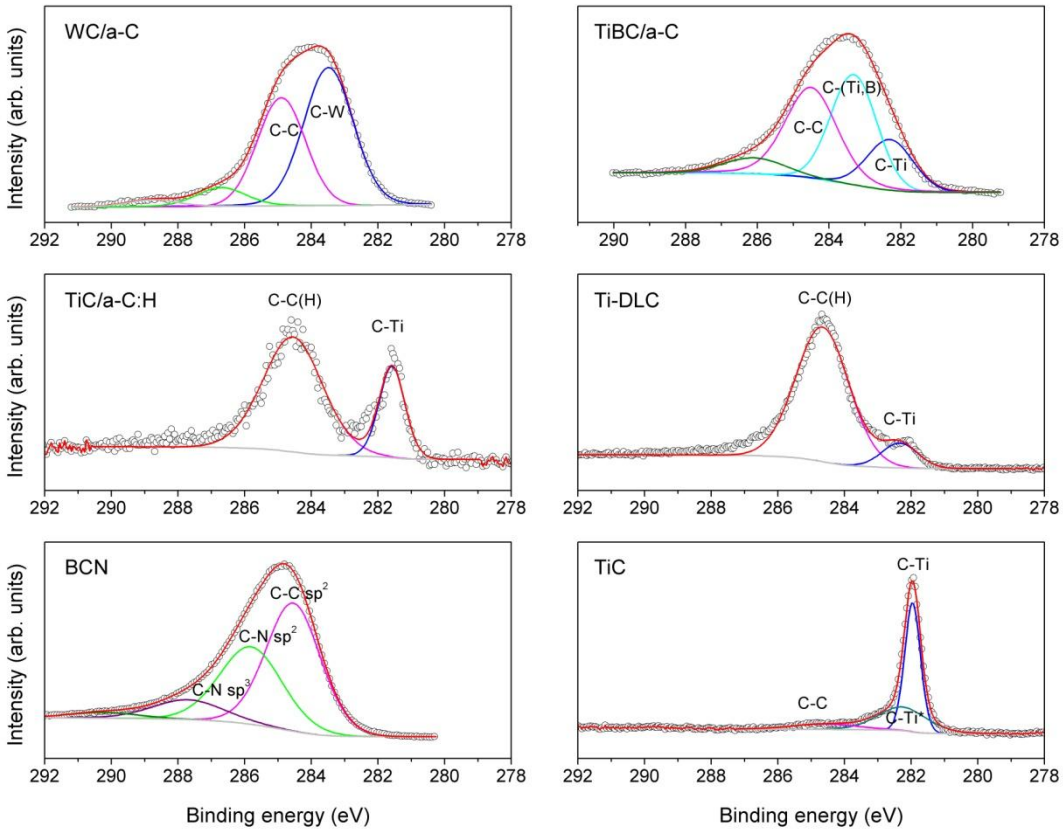

Figure 4

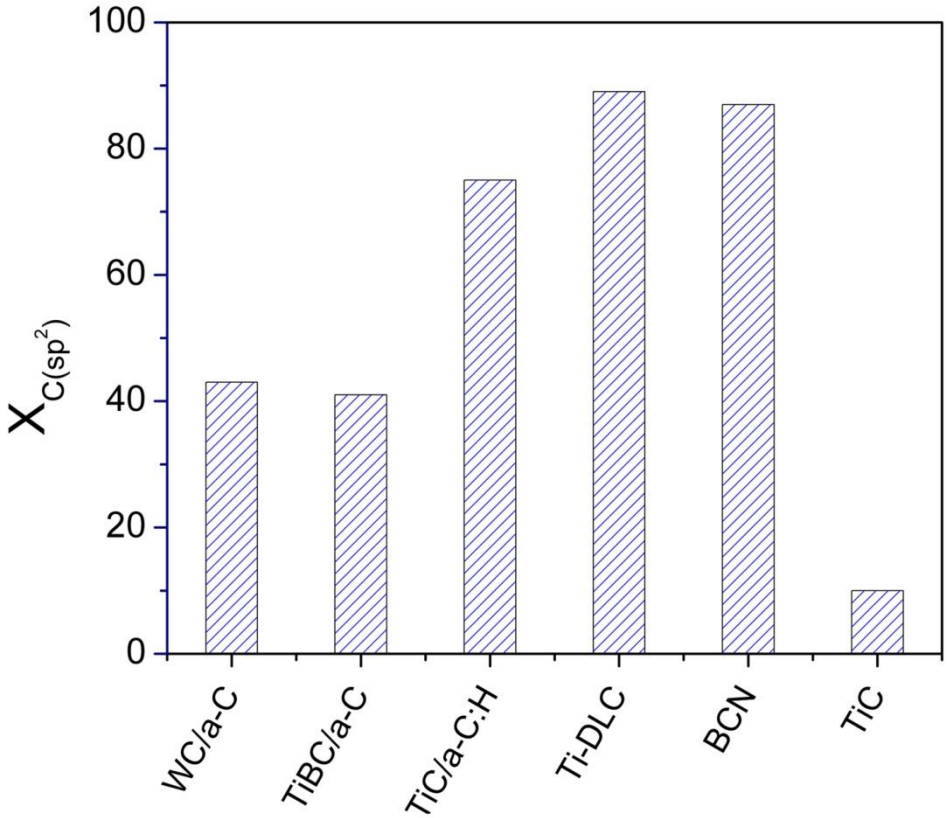

Figure 5

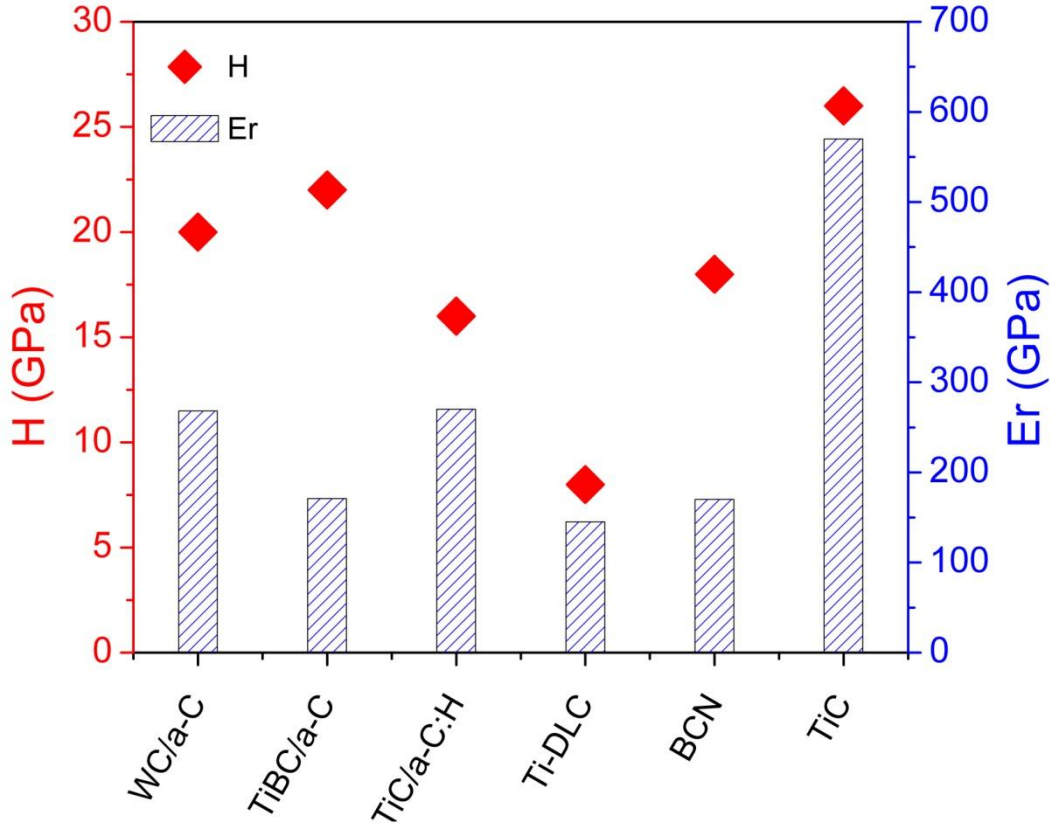

Figure 6

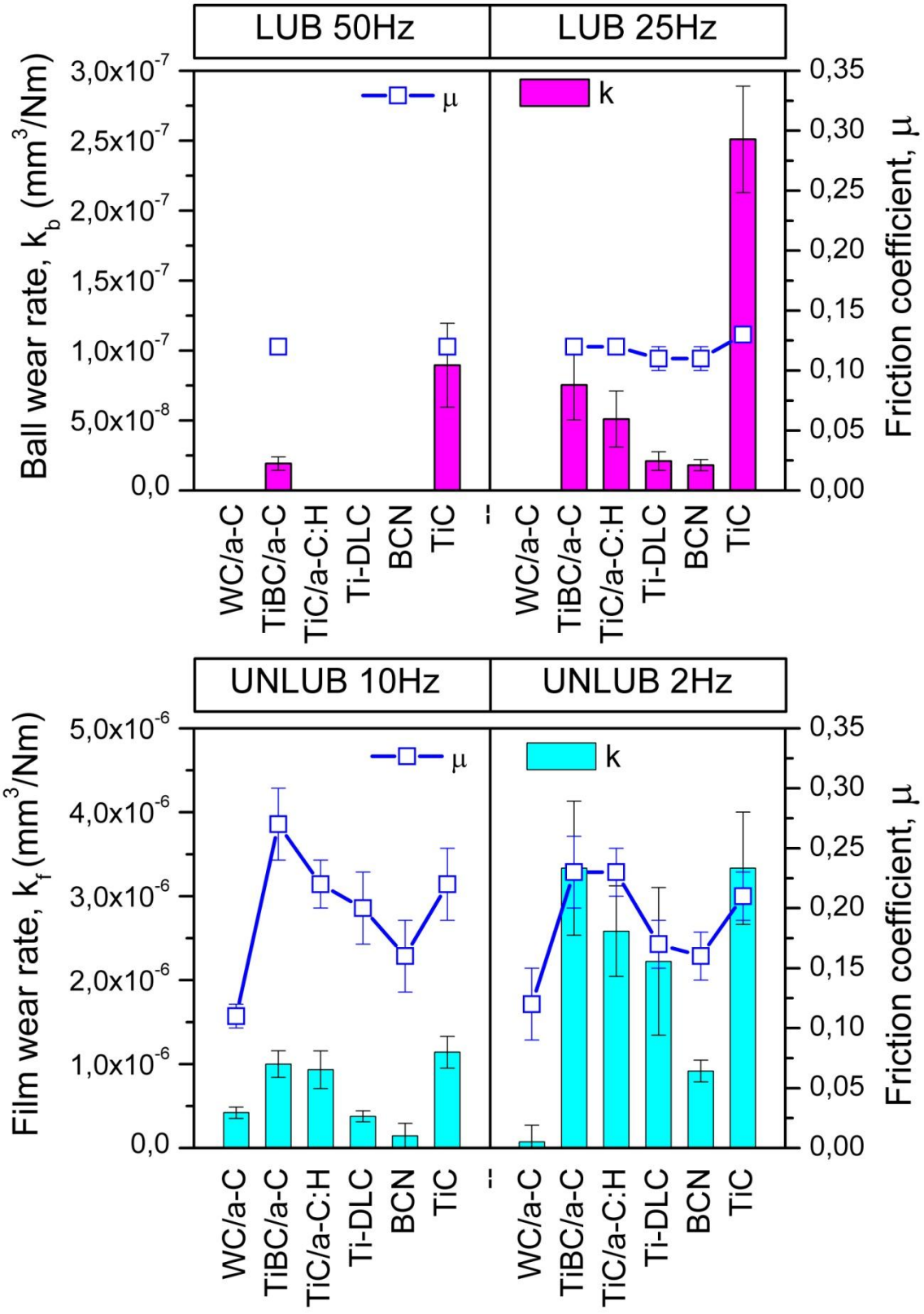

Figure 7

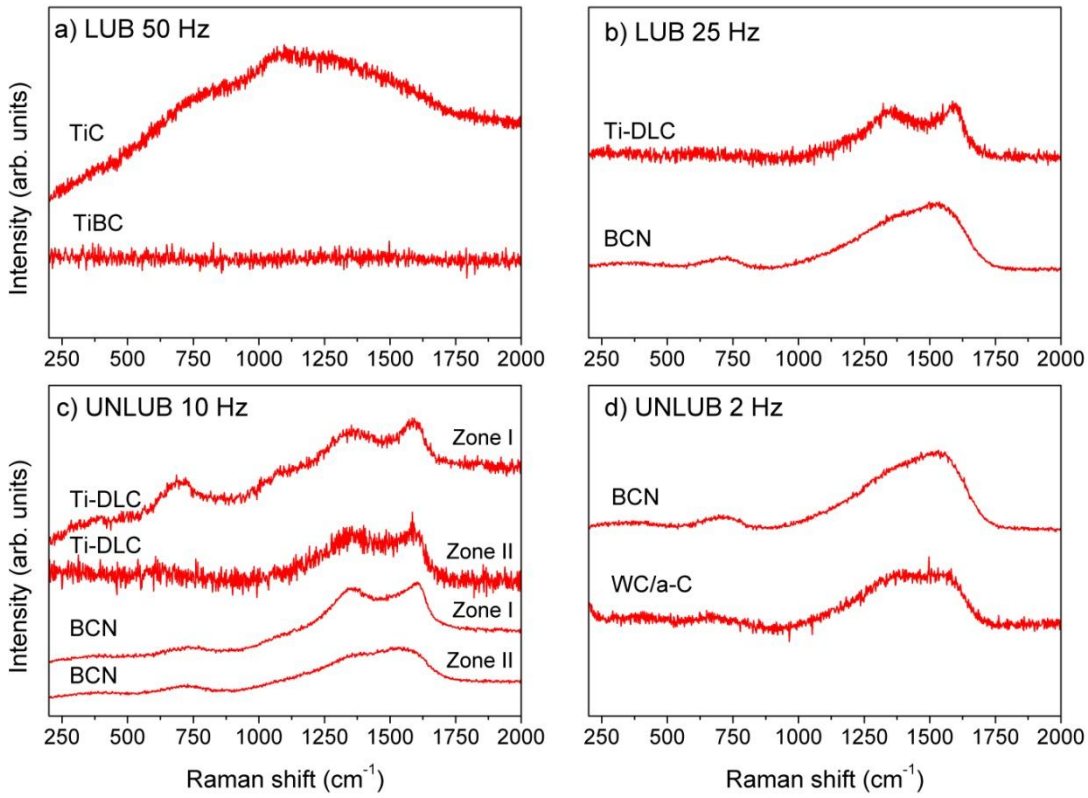

Figure 8

Table 1. C-based coatings used for the SRV tribological study

	WC/a-C	TiBC/a-C	TiC/a-C:H	Ti-DLC	BCN	TiC
Thickness (µm)	1.5	1.5	1.5	2	1.5	1.5
Ra (nm)	0.008	0.029	0.029	0.022	0.011	0.028
Interlayer	W_2C	TiBC	Ti/TiC	Ti	Ti(N)	-
C (at.%)	72	61	54	79	66	45
$X_{C(sp2)}$ (%)	43	41	75	89	87	10
H (GPa)	20	22	16	8	18	26
E (GPa)	268	171	270	145	170	570
XRD crystal size (nm)	1-2	2-3	3-4	amorphous	amorphous	8-12
Microstructure	columnar	dense	columnar	columnar	dense	columnar

Table 2. Testing conditions for the tribological tests performed in the SRV machine

Materials	**Steel type**	**Diameter (mm)**	**Hardness HRC**	**Ra (μm)**
Ball	100Cr6	10	60 ± 2	0.025
Disks	M2	24	63± 1	0.006
Lubricant	SuperSyn Mobil 5W50			
Coatings	Film characteristics described in Table 1			
Test Conditions	**Lubricated**		**Unlubricated**	
Load (N)	50	20	5	5
Frequency (Hz)	50	25	10	2
Max. Hertzian contact pressure (GPa)	1.7	1.3	0.8	0.8
Stroke (mm)	1	1	2	2
Linear speed (mm/s)	100	50	40	8
Temperature (ºC)	50	50	50	50
Time (min)	30	30	20	15

Highlights

- Comparative tribological behaviour of relevant state-of-the-art carbon-based coatings
- SRV tests were done in C-based films under lubricated and unlubricated conditions
- Higher film hardness is preferable under harsh conditions if contact is lubricated
- High fraction of sp^2-C is more convenient in boundary-lubricated sliding conditions
- WC/a-C, Ti-DLC and BCN films showed the best tribological response in dry sliding